

Linear Instability of a Zonal Jet on an f Plane*

NATHAN PALDOR⁺ AND MICHAEL GHIL

*Department of Atmospheric Sciences and Institute of Geophysics and Planetary Physics,
University of California, Los Angeles, Los Angeles, California*

(Manuscript received 29 September 1995, in final form 8 April 1997)

ABSTRACT

The linear instability of a zonal geostrophic jet with a \cosh^{-2} meridional profile on an f plane is investigated in a reduced-gravity, shallow-water model. The stability theory developed here extends classic quasigeostrophic theory to cases where the change of active-layer depth across the jet is not necessarily small. A shooting method is used to integrate the equations describing the cross-stream structure of the alongstream wave perturbations. The phase speeds of these waves are determined by the boundary conditions of regularity at infinity. Regions exist in parameter space where the waves that propagate along the jet will grow exponentially with time. The wavelength of the most unstable waves is $2\pi R$, where R is the internal deformation radius on the deep side, and their e -folding time is about 25 days.

The upper-layer thickness of the basic state in the system has a spatial structure resembling that of the isopycnals across the Gulf Stream. The unstable waves obtained in the present analysis have a wavelength that is in agreement with some recent observations—based on infrared imaging of the sea surface temperature field—of the fastest-growing meanders' wavelength. Calculated growth rates fall toward the low end of the range of values obtained from these infrared observations on the temporal evolution of Gulf Stream meanders.

1. Introduction

The Gulf Stream system is one of the oceans' most important and striking features (Stommel 1965). Numerous observational, numerical, and theoretical studies have been dedicated to it. Recently, Huang and Stommel (1990) proposed a simplified, steady-state, uniform potential vorticity model that successfully reproduces some of the main features associated with the cross section of the Gulf Stream. In their model, each of several (two or three in the cases studied) discrete isopycnal layers has a uniform value for the potential vorticity (PV), while the flow in each layer is in geostrophic balance with the slope of the interfaces separating the layers. Huang and Stommel calculated only the steady flows and interface depth profiles in their model.

In the present work we address the temporal evolution of small amplitude perturbations for a simple steady-state zonal jet with a meridional profile similar to those studied by Huang and Stommel (1990). The simplest model, which

we treat here, is that of an upper layer of lighter, moving water that overrides a layer of motionless, heavier water. The depth of the interface separating these two layers varies in the cross-stream direction and this depth variation is balanced geostrophically by the flow in the upper layer. Although the PV (potential vorticity) in the upper layer is not uniform in the present study, we assume a profile of the interface separating the two layers in the basic state very similar to the one obtained by Huang and Stommel for the case when the PV is uniform there.

All the profiles studied by Huang and Stommel are characterized by two or more moving isopycnal layers, each of them having its own uniform PV. The stability of such a model flow is more cumbersome to investigate and the simpler model of a single moving layer, studied in the present work, is a prototype case that can serve as an initial step toward the stability analysis of Huang and Stommel's more elaborate profiles. Unlike in frontal problems (e.g., Paldor 1983; Cushman-Roisin et al. 1993), the interface separating the two layers in the present study does not outcrop; this fact simplifies the analysis by removing the singularity associated with the outcrop.

A closely related instability problem—in which each of several isopycnal layers has piecewise-uniform PV, that is, each layer contains meridional bands in which the PV is uniform—was studied by Meacham (1991). In the simplest of Meacham's cases, the lower one of the two layers is not banded and the PV there is uniform throughout. In the upper layer, on the other hand, the

* Institute of Geophysics and Planetary Physics Contribution Number 4606.

⁺ Permanent affiliation: Department of Atmospheric Sciences, The Hebrew University of Jerusalem, Jerusalem, Israel.

Corresponding author address: Dr. Michael Ghil, Institute of Geophysics and Planetary Physics, University of California, Los Angeles, 405 Hilgard Avenue, Los Angeles, CA 90095-1567.
E-mail: ghil@atmos.ucla.edu

PV has a jump along a line called the front. This PV front has no corresponding density jump and the latter remains uniform throughout the layer.

Since the PV in the lower layer is uniform in Meacham's model, there has to be a mean flow there (to compensate for the varying thickness of this layer) and the flow velocity grows linearly with distance from the front. Thus, the mean velocities in both layers tend to infinity in the cross-stream direction: As one moves away from the PV front, which generates the flow in the two layers, these flows are becoming ever stronger. Despite of the infinite shear that exists between the two layers, there are no instabilities and all perturbations remain finite at all times in this particular version of Meacham's model (while in other cases instabilities do exist). By contrast, we will show that in our model, where the velocities in the mean state are finite, instabilities exist and are characterized by a fairly realistic wavelength of the fastest growing perturbation.

We expect a limiting case of the present study, when the ratio of the upper-layer depths on either side of the jet approaches unity, to agree with quasigeostrophic (QG) theory. In this limit we expect, therefore, the flow to be stable (to barotropic perturbations) unless the velocity profile contains an inflection point (Kuo 1949; Pedlosky 1987). At some value of the depth ratio, however, QG theory will lose its validity and instabilities might develop even when the velocity profile is stable according to QG theory.

The present study is organized as follows. In section 2, the mathematical model is formulated. The linear stability problem is solved in section 3. Results are compared with observations and other theories in section 4.

2. Formulation of the problem

a. The mean state

We envisage a steady zonal jet flowing on an f plane in the upper layer of a two-layer ocean as shown in Fig. 1. In the lower layer the mean flow vanishes and, since this layer is assumed to be infinitely deep, the PV there vanishes too. The flow in the upper layer is in geostrophic balance with the prescribed slope of the interface separating the two layers; the PV in the upper layer is not prescribed a priori, as in other studies, being determined instead from the geostrophic velocity there and the interface depth. The equations describing the mean flow are closed by specifying the cross-stream variation of the interface.

Following the results of Huang and Stommel (1990) for the case where two layers have prescribed constant, nonzero PV and nonzero velocity, we let the nondimensional interface depth $\bar{h}(y)$ vary as

$$\bar{h}(y) = \frac{1}{2}(1+r) - \frac{1}{2}(1-r)\tanh(ay). \quad (1)$$

The dimensional height H of the upper layer on the deep

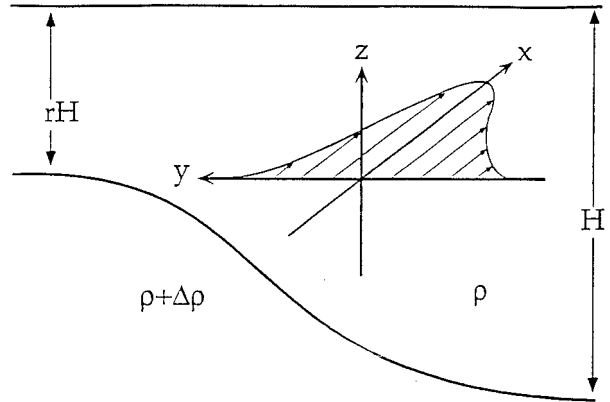


FIG. 1. The cross-stream profile of the assumed zonal jet's interface between the upper and lower layer and the zonal velocity profile in geostrophic balance with it. The parameter a determines the rate (in units of deformation radius) at which the interface shoals from its depth at $-\infty$ to that at $+\infty$, while $r < 1$ is the interface depth on the shallow side measured in units of the deep side's depth.

side, at $y \rightarrow -\infty$, has been used as the height scale and rH is the depth on the shallow side, $y \rightarrow +\infty$. The parameter a in Eq. (1) determines the (nondimensional) slope of the interface depth near $y = 0$, which equals

$$-\frac{1}{2}(1-r)a$$

at $y = 0$. The scale for the horizontal coordinates x and y is the Rossby radius of deformation $\sqrt{g'H/f}$, where g' is the reduced gravity (i.e., the gravitational acceleration multiplied by the fractional density difference between the two layers) and f is the Coriolis parameter.

Given the depth profile (1), the geostrophic velocity for the jet in the upper layer, $\bar{u}(y)$, is given by

$$\bar{u}(y) = -\bar{h}_y(y) = \frac{1-r}{2}a \frac{1}{\cosh^2(ay)}; \quad (2)$$

this yields a zonally flowing jet, symmetric about $y = 0$. The velocity scale used here is the length scale described above (i.e., the internal deformation radius) divided by the natural timescale of $f^{-1} = [4\pi \sin(\text{lat})]^{-1} \times 24 \text{ h}$.

b. Linear stability problem

We now linearize the x and y momentum equations as well as the continuity equation in the upper layer about the mean profile $\bar{h}(y)$ and flow $\bar{u}(y)$ given by Eqs. (1), (2). We let the dependence on x and t of all the perturbation variables— u , v , and h —be the typical one for a zonally propagating plane wave, $\exp[ik(x - ct)]$. After some trivial simplifications, which include the elimination of u , this yields the following coupled ordinary differential equations for the y -dependent amplitude of h and $V \equiv -iv/k$:

$$h_y = V \left(k^2(\bar{u} - c) - \frac{1 - \bar{u}_y}{\bar{u} - c} \right) + h \left(\frac{1}{\bar{u} - c} \right), \quad (3)$$

$$V_y = V \left(\frac{\bar{u}}{h} - \frac{1 - \bar{u}_y}{\bar{u} - c} \right) + h \left(\frac{1}{\bar{u} - c} - \frac{\bar{u} - c}{h} \right). \quad (4)$$

In the absence of outcropping of the interface, the only boundary conditions of interest for these equations are regularity at infinity, as no other singular points exist for unstable modes, for which $\text{Im}(c) \neq 0$. By contrast, stable modes have an additional singularity at the critical layers where $\bar{u} - c = 0$. These modes are of interest in the present context only to the extent that the concept of overreflection (e.g., Lindzen and Barker 1985) suggests that they play a physical role in inducing the instability, albeit indirectly.

The infinite y domain can be transformed into a finite one by observing that $\bar{h}(y)$ is monotonic and using it to replace y as the independent variable. Defining

$$z = \frac{\bar{h}(y) - r}{1 - r} \quad (5)$$

maps the points $y = -\infty$, $y = +\infty$, and $y = 0$ into $z = 1$, $z = 0$, and $z = \frac{1}{2}$, respectively. Both \bar{h} and \bar{u} can be expressed as functions of z ;

$$\bar{h}(z) = r + (1 - r)z, \quad (6)$$

$$\bar{u}(z) = 2a(1 - r)z(1 - z). \quad (7)$$

Meridional differentiation transforms according to

$$\frac{\partial}{\partial y} = -\frac{\bar{u}}{1 - r} \frac{\partial}{\partial z}, \quad (8)$$

so that the governing differential equations for $h(z)$ and $V(z)$ become

$$-\frac{\bar{u}}{1 - r} h_z = V \left(k^2(\bar{u} - c) - \frac{1 - \bar{u}'}{\bar{u} - c} \right) + h \left(\frac{1}{\bar{u} - c} \right), \quad (9)$$

$$-\frac{\bar{u}}{1 - r} V_z = V \left(\frac{\bar{u}}{r + (1 - r)z} - \frac{1 - \bar{u}'}{\bar{u} - c} \right) + h \left(\frac{1}{\bar{u} - c} - \frac{\bar{u} - c}{r + (1 - r)z} \right), \quad (10)$$

where \bar{u}' on the right-hand side (rhs) of (9), (10) is the shear of the mean velocity expressed in the z coordinate [which differs from \bar{v}_y by the factor $-\bar{u}/(1 - r)$]. The system (9), (10) constitutes a nonlinear eigenvalue problem in the phase velocity c for which boundary conditions at the end points $z = 0$ and $z = 1$ are required. These end points coincide with the singular points, where $\bar{u}(z)$ vanishes. Given the algebraic nature of the singularity at these points, an expansion about them can remove the singularity and identify the behavior of the regular solutions there.

The expansion of $\bar{u}(z)$ near the two end points yields

$$\bar{u}(\epsilon) = \bar{u}(0) + \bar{u}_z(0)\epsilon = 2a(1 - r)\epsilon, \quad (11)$$

$$\bar{u}(1 - \epsilon) = \bar{u}(1) + \bar{u}_z(1)(-\epsilon) = 2a(1 - r)\epsilon. \quad (12)$$

Thus, near $z = 0$ in particular, the governing equations take the form

$$-2a\epsilon h_\epsilon = \left(-k^2c + \frac{1}{c} \right) V + \left(-\frac{1}{c} \right) h + O(\epsilon), \quad (13)$$

$$-2a\epsilon V_\epsilon = \left(\frac{1}{c} \right) V + \left(-\frac{1}{c} + \frac{c}{r} \right) h + O(\epsilon). \quad (14)$$

For the regular solution we let

$$h \sim A\epsilon^\alpha, \quad (15)$$

$$V \sim B\epsilon^\alpha \quad (16)$$

near $z = 0$ and require $\text{Re}(\alpha) > 0$ for regularity, with A and B constants to be determined; the linearity of the problem allows us to let one of these constants equal 1. Substituting the asymptotic expressions (15) and (16) for h and V in Eqs. (13), (14), we get two linear equations for A and B :

$$\left(\frac{1}{c} - 2a\alpha \right) A + \left(k^2c - \frac{1}{c} \right) B = 0, \quad (17)$$

$$\left(\frac{c}{r} - \frac{1}{c} \right) A + \left(\frac{1}{c} + 2a\alpha \right) B = 0. \quad (18)$$

For a nontrivial solution, that is, $|A|^2 + |B|^2 \neq 0$, the determinant of this 2×2 system has to vanish. This determines α as

$$\alpha = \pm \frac{1}{2a} \sqrt{k^2 + \frac{1}{r} - \frac{k^2c^2}{r}}, \quad (19)$$

where the sign is chosen such that $\text{Re}(\alpha) > 0$ even for complex c so that the solution will be regular at $z = 0$. For this value of α , the constants A and B are related by

$$\frac{B}{A} \equiv \frac{V(0)}{h(0)} = \frac{2a\alpha - 1/c}{k^2c - 1/c}. \quad (20)$$

A similar analysis near $z = 1$ reveals that the regular solutions there vary as $(1 - z)^\beta$, where

$$\beta = \pm \frac{1}{2a} \sqrt{1 + k^2 - k^2c^2} \quad (21)$$

and, here too, the sign is chosen such that $\text{Re}(\beta) > 0$. For this value of β we get

$$\frac{V(1)}{h(1)} = \frac{1 - c^2}{1 - 2ac\beta}. \quad (22)$$

The governing equations (9), (10), along with the asymptotic expansions (19)–(22) of the regular solutions near the singular points $z = 0$ and $z = 1$, are solved in the next section as an eigenvalue problem: h and V are the eigenfunctions and the phase speed c is the corresponding eigenvalue.

3. Unstable waves

The possibly complex values of the phase speed c are determined, for given r and k , by solving the eigenvalue problem formulated in the previous section. The method presented here is a slight variation on the more general scheme described in Paldor and Ghil (1991). Briefly, the system (9), (10) is integrated first starting from some $z = \epsilon$, say $\epsilon = 10^{-5}$, to $z = 1/2$ by letting $h(\epsilon) = \epsilon^\alpha$, where α is given by (19) and $V(\epsilon)$ by $h(\epsilon) \times$ [rhs of (20)]. The values of $h^-(1/2)$ and $V^-(1/2)$ as obtained from this integration are stored. Another integration is now carried out from a point $z = 1 - \epsilon$ to $z = 1/2$ by letting $h(1 - \epsilon) = \epsilon^\beta$ and $V(1 - \epsilon) = h(1 - \epsilon) \times$ [rhs of (22)]. The values of $h^+(1/2)$ and $V^+(1/2)$ from this integration are also stored.

The numerical solutions of the perturbation equations have to be continuous across $z = 1/2$ in order for them to be acceptable physically. One can always make one of the two functions, $h(z)$ say, continuous at $z = 1/2$ by multiplying the functions found previously in $z = (1/2, 1)$ by the numerical factor $h^-(1/2)/h^+(1/2)$. The value of c is determined by requiring that the other function, $V(z)$ in this case, be also continuous at $z = 1/2$ [i.e., after the function $V^+(z)$ has been multiplied by the same numerical factor as $h^+(z)$]. The values of c that satisfy this requirement are therefore the zeroes of

$$F(c; k, r, a) \equiv V^+\left(\frac{1}{2}\right) \times h^-\left(\frac{1}{2}\right) - V^-\left(\frac{1}{2}\right) \times h^+\left(\frac{1}{2}\right). \quad (23)$$

Many real eigensolutions exist but are of no physical interest here, as explained in the previous section, after Eqs. (3), (4). Therefore, only eigenvalues with $\text{Im}(c) \neq 0$ are described below.

Typical results for the growth rate kc_i and the phase speed c_r as a function of the wavenumber k are shown in Fig. 2 for $a = 1$ and for $r = 0.5$ and 0.9 . The overall shape of the instability curves in the two cases is very similar: Both kc_i and c_r are zero as $k \rightarrow 0$ and increase quadratically with wavenumber for small k . The growth rate has a maximum near $k = 1.0$, that is, for a wavelength of $2\pi R$ in dimensional units, and becomes zero again (linearly) at $k = k_0(a, r) < 2$. The phase speed keeps increasing roughly linearly with k .

Two differences should be noted, however, between Figs. 2a and 2b: First, for $r = 0.5$ the maximum growth rate is 6×10^{-3} , while for $r = 0.9$ it is only 2.3×10^{-3} ; the difference between the phase speed values is even more pronounced. Second, the cutoff value, above which no instabilities can be found, is higher for $r = 0.9$. Recalling from Eq. (7) that the mean speed \bar{u} is proportional to $(1 - r)$, it follows that the more energetic jets have a larger instability exponent but the instability is restricted to a narrower wavenumber range.

The dependence of the instability exponent kc_i on the depth ratio r —for fixed wavenumber k —is shown in

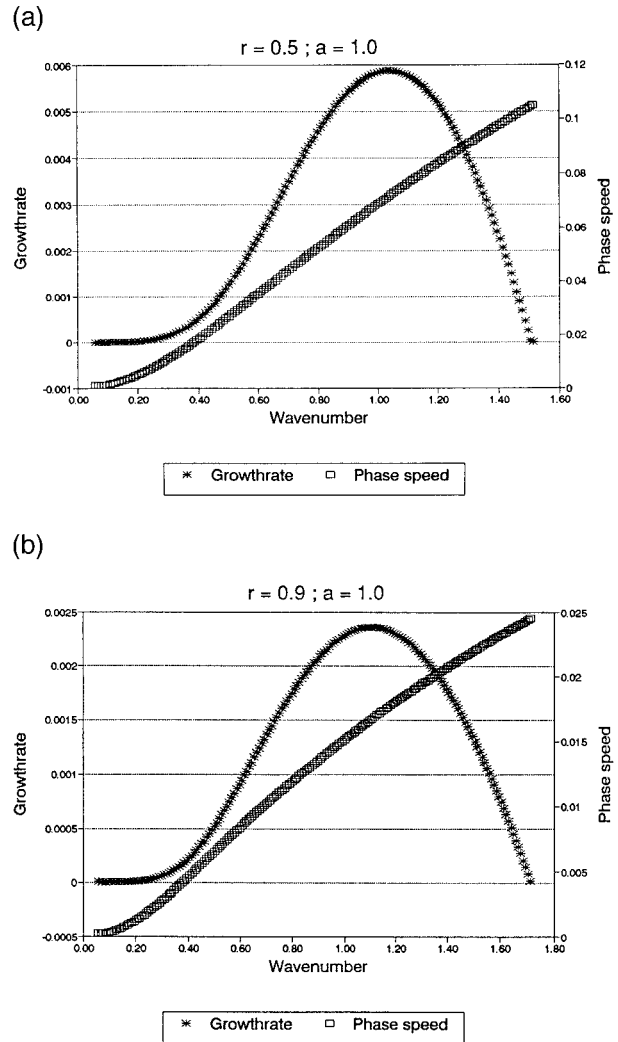


FIG. 2. The growth rate $kc_i(k)$ and the phase speed $c_r(k)$, for (a) $r = 0.5$ and (b) $r = 0.9$; $a = 1.0$ in both cases.

Figs. 3a and 3b for $k = 1.0$ and $k = 1.5$, that is, near the wavenumber of maximal growth. As expected, the growth rate vanishes at $r = 1.0$, where there is no jet at all. Surprisingly, however, as long as $(1 - r)$ does not vanish, the instability exponents are different from 0 and, in fact, the curves seem to be linear with $(1 - r)$ as $(1 - r) \rightarrow 0$. Since at r values near 1 the depth variations relative to the mean depth of the interface are small and so the QG theory is expected to be valid, the instability found here can be regarded as a continuation of the QG instability into the regime where the relative depth variations are not necessarily small. The differences between QG theory and the present one are discussed in section 4a below.

At the other end, of vanishing depth on the shallow side of the jet, a cutoff exists in r at some $r_0 > 0$, beyond which the jet is stable for all $0 < r < r_0$. These numerical findings will be addressed in the next section in the context of QG theory and of PV profile considerations.

An example of the eigenfunctions associated with the eigenvalues presented above is shown in Fig. 4. The eigenfunctions do indeed both vanish at the end points $z = 0, 1$, which correspond to $y = \pm\infty$, and are continuous at $z = 1/2$ where the velocity is maximum—as required. The similarity between the V and h eigenfunctions, in both their real and imaginary parts, is expected for the eigenvalues used in Fig. 4. Indeed, in the limit of small c , the exponents at both ends satisfy

$$\alpha = \frac{1}{2a}\sqrt{k^2 + \frac{1}{r}} + O(c), \tag{24}$$

$$\beta = \frac{1}{2a}\sqrt{k^2 + 1} + O(c), \tag{25}$$

and

$$\frac{V(0)}{h(0)} = 1 + O(c) = \frac{V(1)}{h(1)}. \tag{26}$$

Hence, for small c values we do expect the V and h eigenfunctions to be similar. Comparing Fig. 4a ($|c| = 0.0692$) with Fig. 4b ($|c| = 0.0152$), it is clear that these functions become less similar as $|c|$ increases.

4. Discussion

a. Potential vorticity considerations

The results presented in the last section regarding the range in r over which the jet is unstable can be related to the PV distribution in the upper layer. The latter is given, in the z coordinate, by

$$Q(z) = \frac{1 + 4a^2(1 - r)z(1 - z)(1 - 2z)}{r + z(1 - r)} \tag{27}$$

so that

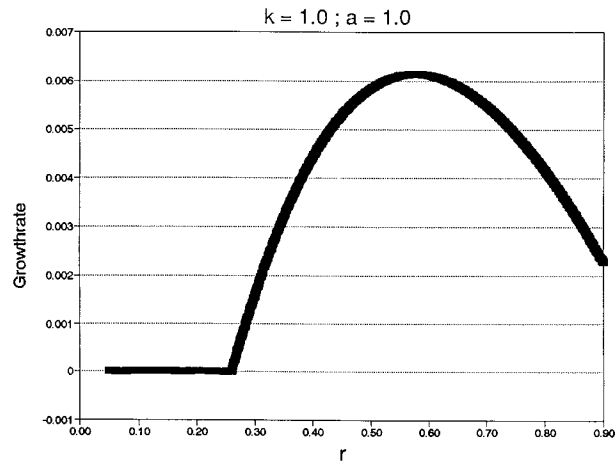
$$Q(0) = \frac{1}{r}, \quad Q\left(\frac{1}{2}\right) = \frac{1}{(1 + r)/2}, \quad Q(1) = 1. \tag{28}$$

The condition $r < 1$ implies that $Q(z)$ has to decrease overall as z goes from 0 to 1, $Q(0) > Q(1/2) > Q(1)$. Moreover, inspection of Eq. (27) reveals that in the inner region, near the core of the jet at $z = 1/2$, the gradient of $Q(z)$ is always negative when $r < 1$. This decrease of $Q(z)$, however, is not necessarily monotonic throughout the interval $(0, 1)$ and the gradient of $Q(z)$ can, in particular, be positive near the end points $z = 0, 1$ for certain values of a and r . It follows that, in such cases, the PV will have inflection points near *one or both* end points. The conditions for $Q_z(z)$ to be positive near these end points are determined as follows: Near $z = 1$ (that is, $y = -\infty$), we find that

$$Q_z(1) = (1 - r)(4a^2 - 1), \tag{29}$$

which is positive for all $a > 1/2$ and $r < 1$, while near $z = 0$ (that is, $y = +\infty$)

(a)



(b)

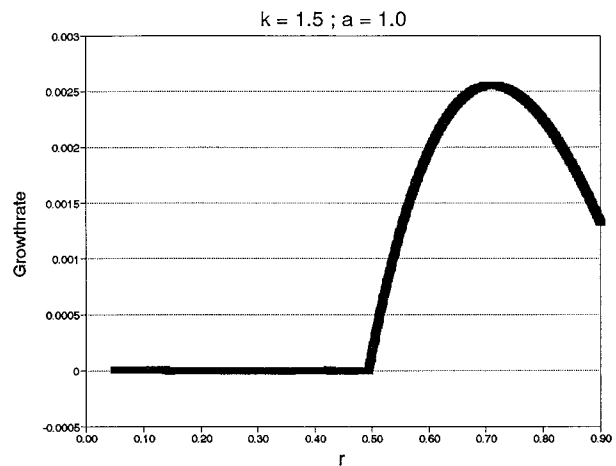


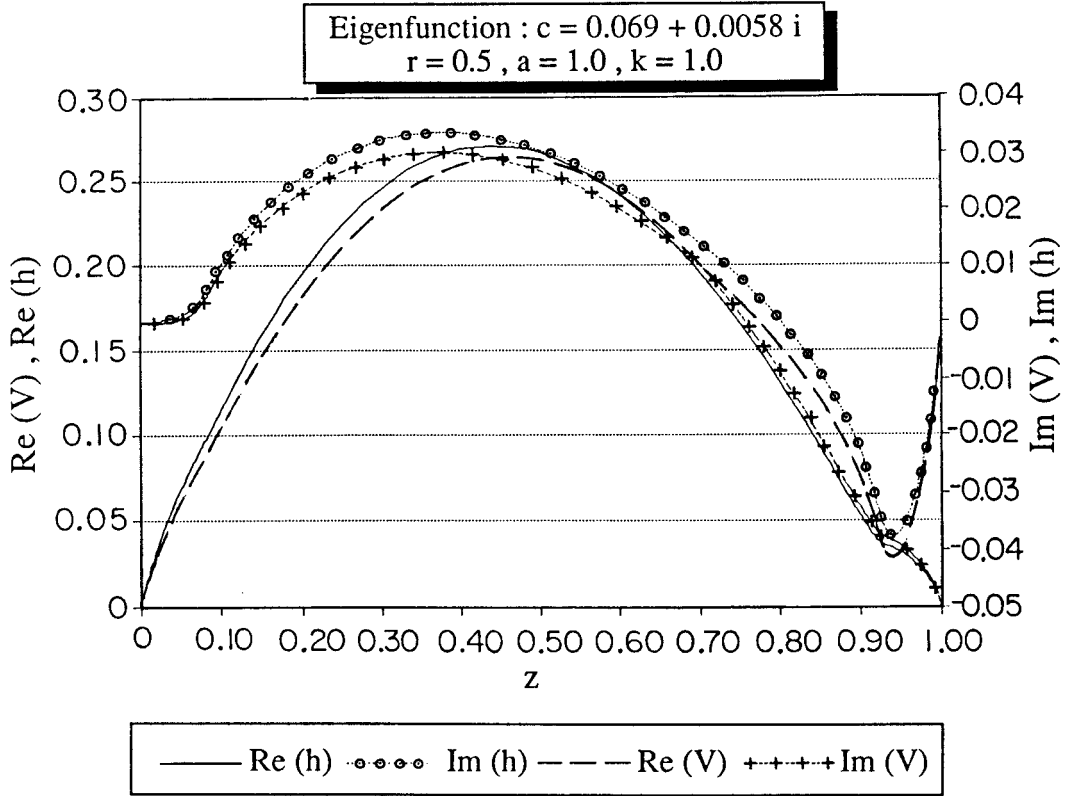
FIG. 3. The dependence of the instability exponent kc_i on the depth ratio r for (a) $k = 1.0$ and (b) $k = 1.5$; $a = 1.0$ in both cases.

$$Q_z(0) = \frac{(1 - r)(4a^2r - 1)}{r^2}, \tag{30}$$

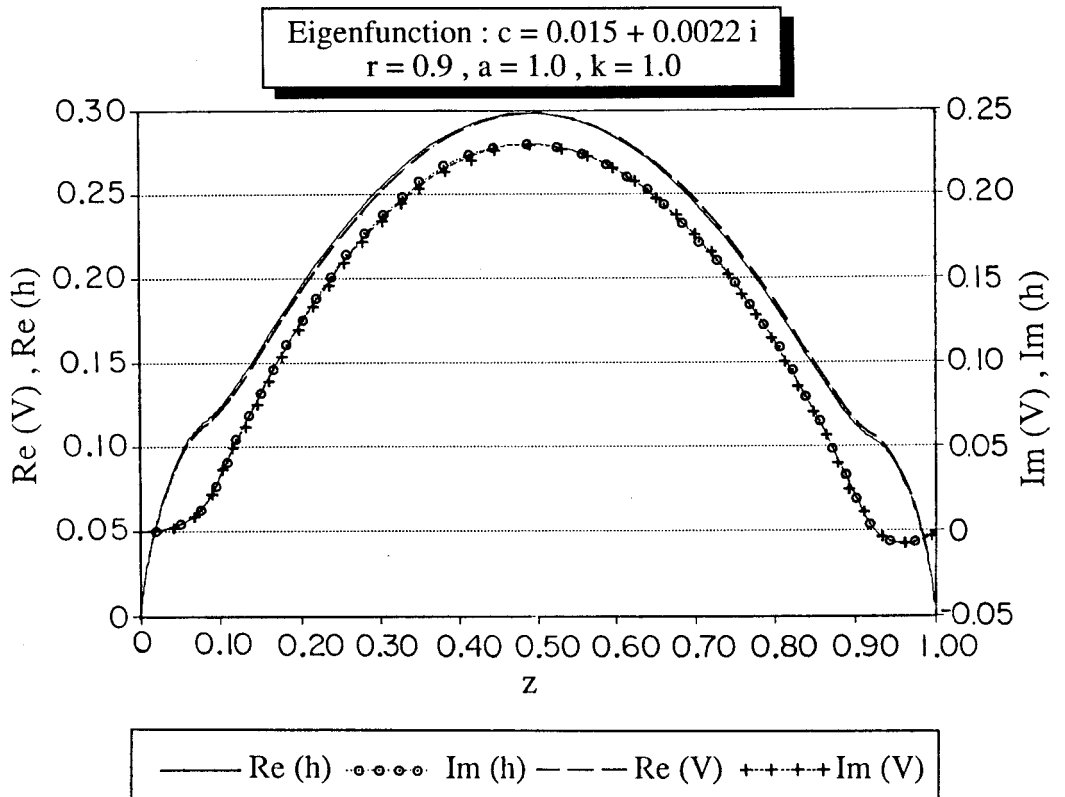
which is positive for all $1 > r > 1/4a^2$. The latter condition is more restrictive than the former; that is, a positive value of (30) implies a positive value of (29): if $Q_z(z)$ is positive at the shallow end point, it has to be so at the deep end.

In order for the PV gradient in the upper layer to change sign, $Q_z(z)$ has to change sign there too since $Q_y(y)$ differs from $Q_z(z(y))$ by factors of a constant sign only [cf. Eq. (8)]. According to QG theory, a single extremum of $Q(y)$ is necessary to yield instability; this will occur near the deep end of the jet ($z = 1$) provided $a < 1/2$ and regardless of the value of r . In Fig. 3, however, where the dependence of growth rate on r is shown for k values that yield near-optimal growth and for $a =$

(a)



(b)



1, there is a (k dependent) cutoff value r_0 of r below which there is no instability; in Fig. 3b, this cutoff value is $r_0 \approx 0.28$. We notice, on the other hand, that on the shallow side of the jet, at $z = 0$ ($y = +\infty$), we have $Q_z > 0$ and hence an inflection point of $\bar{u}(z)$ in the interval $0 < z < 1/2$, provided $r > 1/4a^2$ or $r > 0.25$ for $a = 1$. This PV consideration, along with the numerical result above, together suggest that—for the present model—a second inflection point is necessary for the instability to obtain.

This requirement of a second inflection point does not contradict QG theory, which stipulates merely that one such point is necessary—but not sufficient—for an instability to occur. In the present problem, the jet's physical symmetry with respect to the axis ($y = 0$), on the one hand, and the inflection point's occurrence necessarily off this axis—in z as well as y —on the other, imply that there have to be *two* inflection points on the shallow and the deep side, rather than one only.

Equations (29), (30) also suggest that the jet is stable for all r provided $a < 1/2$. Further analysis of Eq. (27) confirms that the PV gradient in the upper layer is then of one sign. Our numerical results have confirmed this stability conjecture inspired by QG theory: no instabilities were found when $a < 1/2$ for a wide range of wavenumbers and depth ratios. An example of the dependence of the instability exponents on the jet's width parameter a is shown in Fig. 5 for $r = 0.5$ and 0.9 and for $k = 1$. For both r values, a cutoff a_0 in a occurs just below $a = 1$.

Griffiths et al. (1982) and Ripa (1983) have demonstrated that in certain primitive equation models, where the QG approximation is no longer valid, instabilities do arise even when the QG necessary conditions for instability do not hold. In the study of Griffiths et al. outcropping of isopycnals occurs, while Ripa studied instability on a β plane. In the present study, the f -plane approximation is made and no outcropping occurs. Boss et al. (1996) demonstrated that, in fact, a surface of discontinuity can restore the applicability of the QG theory, so the QG necessary conditions still hold even though the relative change in the upper layer's depth is $O(1)$.

For $a > a_0$, the growth rate increases linearly with $a - a_0$. This linear dependence implies that the instability owes its existence to the horizontal shear in the jet, as in QG theory's barotropic instability (Pedlosky 1987). Kuo's (1949) classic analysis of a jet's instability in the QG barotropic setting, however, yields a growth rate kc_i of the order of $0.05\bar{u}_{\max}$, ignoring the details of the jet's velocity profile $\bar{u} = \bar{u}(y)$. In our model, Eq. (2) gives $\bar{u}_{\max} = a(1 - r)/2 \approx 0.25$, for $a = 1$ and $r = 0.5$. This would yield a QG growth rate, according to Kuo, of

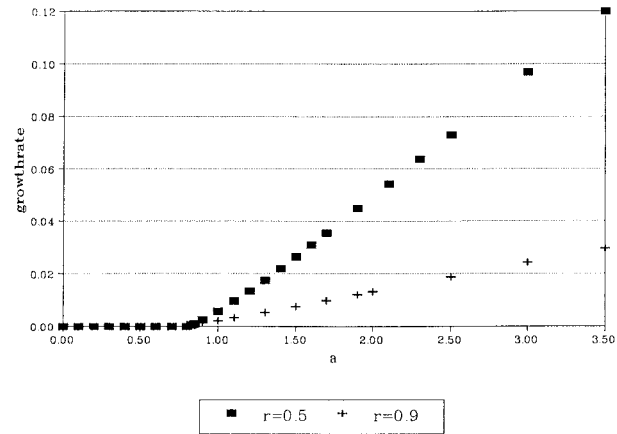


FIG. 5. The dependence of the growth rate on the jet's width for $k = 1$ and r values of 0.5 (full rectangles) and 0.9 (plus signs). For the latter, growth rates are uniformly lower (compare also Fig. 2).

0.0125, about twice as large as the largest kc_i found in the present study for $a = 1.0$ (see Fig. 2a) but smaller QG growth rates than those found here for larger values of a (see Fig. 5).

b. Observations

The Gulf Stream east of Cape Hatteras provides a primary oceanic example of a near-zonal jet. Various field experiments were conducted in the past to determine the length scale and growth rate of rings and eddies that form along it (Robinson 1983).

Several observations concerning the growth of meanders on the Gulf Stream and their wavelength were recently reported in the literature. Watts and Johns (1982) have used moored arrays of inverted echo sounders (IES) to track the wavelength of meanders propagating through the array of moorings. They calculated an e -folding time of 6 days for meanders with wavelengths exceeding 400 km, whose period was about two weeks. Using the same IES instruments but in a different segment of the Gulf Stream, Kontoyiannis and Watts (1994) found meanders with a wavelength of 260 km and a period of 8 days to have a maximal growth rate that corresponds to an e -folding time of about 3 days.

Using 8 years of infrared (IR) satellite imaging, Lee and Cornillon (1996) have calculated that the period and wavelength of the fastest-growing meanders is of about 40 days and 350 km, respectively, while the e -folding time is between 12 and 25 days. The temporal evolution of a single 100-km meander—first noticed in satellite IR images on 15 February 1977 and observed to have detached from the stream into a cold core ring

←

FIG. 4. The complex eigenfunctions $h(z)$ and $V(z)$ that correspond to near-maximal growth rates, $k = 1$, for (a) $r = 0.5$ and $kc_i = 0.0058$ and for (b) $r = 0.9$, $kc_i = 0.0022$.

on 10 March 1977—is described in detail by Richardson (1980).

All these observations point to the fact that more than one instability mechanism may be responsible for the observed growth of wavelike perturbations on the Gulf Stream. In fact, Feliks and Ghil (1996), using a multimode QG model, find two distinct instabilities, short- and long-wave, both with an e -folding time of about 5–7 days; the former instability has wavelengths of about 250 km and periods of about 10 days, the latter 400 km and hundreds of days, respectively. The former are closer to the observations of Kontoyiannis and Watts (1994), the latter to those of Lee and Cornillon (1996). Meacham (1991) also obtained two groups of unstable waves, with wavelengths of 200 and 400 km, both having an e -folding time of about 5 days.

The present 1½-layer model only supports one type of instability. In particular, it cannot capture baroclinic instability, which requires the presence of vertical shear in the horizontal velocity. In a layered model, like the one considered here, this can only occur when the velocity perturbations in the active (upper) layer are coupled with those in the lower (passive) layer. Theoretical models that include baroclinicity (Barth 1994; Fukamachi et al. 1995; Samelson 1993) have shown that the growth rate and wavelength associated with this instability are on the order of a few days and tens of kilometers. The effect of differences in water column stratification on either side of the front was studied by Feliks and Ghil (1997), who found instabilities with growth rates of 5–6 days and wavelength of about 200 km that correspond roughly to the short waves of the Feliks and Ghil (1996) uniform-stratification model.

It is evident that baroclinic instability will dominate the evolution of Gulf Stream meanders at shorter wavelengths and faster growth rates—as inferred from IES measurements (Kontoyiannis and Watts 1994)—especially near the separation of the stream from the coast at Cape Hatteras. The instability studied here, on the other hand, is potentially quite relevant to observations characterized by larger wavelengths and slower growth rates, such as those described by Lee and Cornillon (1996), farther downstream.

Furthermore, linear instability theories, such as ours, are inherently relevant only to the initial stages of a perturbation's evolution, when its amplitude is sufficiently small. By contrast, observations are much more easily carried out on the mature stages of its development, when the particular perturbation can be distinguished clearly from both the basic state and the other perturbations that exist in the observed system. Thus, one can only hope to obtain bounds or order-of-magnitude agreements in a comparison between a linear theory and a set of observations.

To apply our model to actual observations on growth of meanders in the Gulf Stream requires some simplifications of the observed mean flow. The first of these is the two-layer representation of the continuous density

stratification. In the present model the lower one of the two layers has no mean flow. We select a fairly deep isotherm across the Gulf Stream to represent the bottom of the active upper layer. The Pegasus data analyzed by Halkin and Rossby (1985, see their Fig. 10) show that only below 4°C does the downstream velocity component become less than 10% of the maximal upper layer's speed. To match the theoretical interface profile in Eq. (1), we fit a hyperbolic tangent function to the 4°C isotherm shown in Halkin and Rossby's work. This yields a dimensional value of the slope parameter a in Eq. (1) that equals 55–60 km, while the asymptotic depths on the shallow and the deep sides are 770 m and 1500 m. The latter two correspond to a depth ratio $r \approx 0.5$. If we take the density jump between the two layers to be 1.6 σ -units (i.e., a temperature jump of 10°C) then the radius of deformation R falls into the range of 55–60 km as well, which gives a nondimensional value of a in our model of the Gulf Stream that equals 1.0.

The instability mechanism proposed here predicts (see Fig. 2) a wavenumber of fastest growth, which is $k = 1$ for $r = 0.5$ and $a = 1$. This yields a dimensional wavelength for this wave of about $2\pi R$ or 350 km. Such a theoretical value is in good agreement with the 350-km wavelength observed by Lee and Cornillon (1996) for their most unstable meanders. The theoretical growth rate associated with this unstable perturbation is on the order of 0.006, which yields a nondimensional e -folding time of about 160 or, in dimensional units, about 25 days. Lee and Cornillon (1996) give e -folding times of 12–25 days, so that the model value lies at the high end of their observed range.

Acknowledgments. The programming assistance provided by A. Agay of the Hebrew University in expediting the numerical solution of the eigenvalue problem is greatly appreciated. Detailed comments of two anonymous reviewers helped clarify the presentation in several places. This study was funded by Office of Naval Research Grant N00014-93-1-0673 to UCLA and by an Israel Academy of Sciences grant to the Hebrew University of Jerusalem. MG is indebted to the Académie des Sciences, Paris, for its Elf-Aquitaine/C.N.R.S. Chair 1995–96, which facilitated the completion of the work. K. E. Hartman helped with the presentation.

REFERENCES

- Barth, J. A., 1994: Short-wavelength instabilities on coastal jets and fronts. *J. Geophys. Res.*, **99**, 16 095–16 115.
- Boss, E., N. Paldor, and L. Thompson, 1996: Stability of potential vorticity front: From quasi-geostrophy to shallow water. *J. Fluid Mech.*, **135**, 65–84.
- Cushman-Roisin, B., L. Pratt, and E. Ralph, 1993: A general theory for equivalent barotropic thin jets. *J. Phys. Oceanogr.*, **23**, 91–103.
- Feliks, Y., and M. Ghil, 1996: Mixed barotropic-baroclinic eddies growing on an eastward midlatitude jet. *Geophys. Astrophys. Fluid Dyn.*, **82**, 137–171.
- , and —, 1997: Stability of a front separating water masses

- with different stratifications. *Geophys. Astrophys. Fluid Dyn.*, **84**, 165–204.
- Fukamachi, Y., J. P. McCreary Jr., and J. A. Proehl, 1995: Instability of density fronts in layer and continuously stratified models. *J. Geophys. Res.*, **100**, 2559–2577.
- Griffiths, R. W., P. D. Killworth, and M. E. Stern, 1982: Ageostrophic instability of ocean currents. *J. Fluid Mech.*, **117**, 343–377.
- Halkin, D., and T. Rossby, 1985: The structure and transport of the Gulf Stream at 73°W. *J. Phys. Oceanogr.*, **15**, 1439–1452.
- Huang, R. X., and H. Stommel, 1990: Cross sections of a two-layer inertial Gulf Stream. *J. Phys. Oceanogr.*, **20**, 907–911.
- Kontoyiannis, H., and D. R. Watts, 1994: Observations on the variability of the Gulf Stream path between 74°W and 70°W. *J. Phys. Oceanogr.*, **24**, 1999–2013.
- Kuo, H.-I., 1949: Dynamic instability of two-dimensional nondivergent flow in a barotropic atmosphere. *J. Meteor.*, **6**, 105–122.
- Lee, T., and P. Cornillon, 1996: Propagation and growth of the Gulf Stream meanders between 75° and 45°W. *J. Phys. Oceanogr.*, **26**, 225–241.
- Lindzen, R. S., and J. W. Barker, 1985: Instability and wave overreflection in stably stratified shear flow. *J. Fluid Mech.*, **151**, 189–217.
- Meacham, S. P., 1991: Meander evolution on piecewise-uniform, quasi-geostrophic jets. *J. Phys. Oceanogr.*, **21**, 1139–1170.
- Paldor, N., 1983: Linear instability and stable modes of geostrophic fronts. *Geophys. Astrophys. Fluid Dyn.*, **24**, 299–326.
- , and M. Ghil, 1991: Shortwave instabilities of coastal currents. *Geophys. Astrophys. Fluid Dyn.*, **58**, 225–241.
- Pedlosky, J., 1987: *Geophysical Fluid Dynamics*. 2d ed. Springer-Verlag, 710 pp.
- Richardson, P. L., 1980: Gulf Stream ring trajectory. *J. Phys. Oceanogr.*, **10**, 90–104.
- Ripa, P., 1983: General stability conditions for zonal flows in a one-layer model on the β -plane or the sphere. *J. Fluid Mech.*, **126**, 463–489.
- Robinson, A. R., Ed., 1983: *Eddies in Marine Science*, Springer-Verlag, 609 pp.
- , M. A. Spall, and N. Pinardi, 1988: Gulf Stream simulations and the dynamics of ring and meander processes. *J. Phys. Oceanogr.*, **18**, 1811–1853.
- Samelson, R. M., 1993: Linear instability of mixed-layer front. *J. Geophys. Res.*, **98**, 10 195–10 204.
- Stommel, H., 1965: *The Gulf Stream: A Physical and Dynamical Description*, 2d ed. University of California Press, 248 pp.
- Watts, D. R., and W. E. Johns, 1982: Gulf Stream meanders: Observations on propagation and growth. *J. Geophys. Res.*, **87**, 9467–9475.